

Biomolecules and Biomedicine ISSN: 2831-0896 (Print) | ISSN: 2831-090X (Online)

Journal Impact Factor® (2024): 2.2

CiteScore® (2024): 5.2

www.biomolbiomed.com | blog.bjbms.org

The BiomolBiomed publishes an "Advanced Online" manuscript format as a free service to authors in order to expedite the dissemination of scientific findings to the research community as soon as possible after acceptance following peer review and corresponding modification (where appropriate). An "Advanced Online" manuscript is published online prior to copyediting, formatting for publication and author proofreading, but is nonetheless fully citable through its Digital Object Identifier (doi®). Nevertheless, this "Advanced Online" version is NOT the final version of the manuscript. When the final version of this paper is published within a definitive issue of the journal with copyediting, full pagination, etc., the new final version will be accessible through the same doi and this "Advanced Online" version of the paper will disappear.

# **RESEARCH ARTICLE**

Ergünol et al: Sclerostin ab in bone regeneration

# Sclerostin antibody promotes alveolar bone regeneration after tooth extraction

Erdal Ergünol<sup>1</sup>, Rabia Şemsi<sup>2</sup>, Duygu Dayanır<sup>3</sup>, Remzi Orkun Akgün<sup>4</sup>, Okan Ekim<sup>5</sup>, Altay Uludamar<sup>1</sup>, Ayhan Özkul<sup>6</sup>, Aylin Sepici Dinçel<sup>7\*</sup>

<sup>1</sup>Innovation, Education, Consultation and Organization Company, Alter Group, Istanbul, Türkiye;

<sup>2</sup>Department of Medical Biochemistry, Institute of Health Sciences, University of Gazi, Ankara, Türkiye;

<sup>3</sup>Department of Histology and Embryology, Faculty of Medicine, University of Gazi, Ankara, Türkiye;

<sup>4</sup>Department of Anatomy, Faculty of Dentistry University of Çankırı Karatekin, Çankırı, Türkiye;

<sup>5</sup>Department of Anatomy, Faculty of Veterinary Science, University of Ankara, Ankara, Türkiye;

<sup>6</sup>Department of Pathology, Faculty of Veterinary Science, Emeritus, University of Ankara, Ankara, Türkiye;

<sup>7</sup>Department of Medical Biochemistry, Faculty of Medicine, University of Gazi, Ankara, Türkiye.

\*Correspondence to Aylin Sepici Dinçel: <a href="mailto:asepicidincel@gmail.com">asepicidincel@gmail.com</a>.

DOI: https://doi.org/10.17305/bb.2025.12999

#### **ABSTRACT**

Sclerostin is a key inhibitor of the Wnt signaling pathway, functioning by binding to the LRP5/6 receptor. This interaction inhibits beta-catenin expression, resulting in the downregulation of osteogenic markers, which contributes to the promotion of osteoporosis and an increase in osteoclast numbers. The primary objective of this research was to investigate the effects of Scl-ab on bone formation utilizing graft materials in tooth sockets, and to analyze the regulatory interaction between sclerostin and bone tissue through targeted sclerostin inhibition and stimulation of bone formation in tooth extraction sockets following local, single-dose administration. In this study, New Zealand male rabbits (3 months old, weighing 2.5-3 kg) were fully randomized to minimize bias. The experiments were conducted across five groups: a control group, a graft group, and three experimental groups receiving 100%, 75%, and 50% doses of sclerostin antibody (Scl-ab). Calculated doses of Scl-ab were administered alongside the graft material in the extraction sockets, with results assessed at 2 and 4-week intervals. Cone-beam computed tomography indicated that the tooth extraction sockets treated with varying ratios of Scl-ab with graft material exhibited a statistically significant increase in the mean mandibular BV/TV ratio compared to the control and graft groups, with variations based on time and dosage. While bone volume improved over time, the most significant enhancement was observed in the 100% Scl-ab group. Additionally, the administration of different doses of Scl-ab significantly increased trabecular thickness of the alveolar bone compared to both the control (p < 0.001) and graft (p < 0.001) groups, with histological analysis corroborating these findings. The therapeutic application of Scl-ab facilitates early bone formation, and the localized inhibition of sclerostin secreted within the bone microenvironment targets potential bone regeneration.

**Keywords:** Sclerostin-ab, bone regeneration, graft material.

#### INTRODUCTION

Extensive research in bone biochemistry has identified the Wnt/ $\beta$ -catenin pathway as a pivotal signaling cascade in skeletal physiology. This pathway involves various cellular processes, including embryonic development, tissue homeostasis, and bone metabolism<sup>1,2</sup>. Specifically, the Wnt/ $\beta$ -catenin pathway facilitates osteoblast differentiation, proliferation, and bone matrix synthesis, all of which are fundamental to bone formation. Its regulatory function in coordinating the balance and timing of bone resorption and formation during the remodeling cycle has made the pathway a major pharmacological target in skeletal disorders.

The Wnt/ $\beta$ -catenin pathway is tightly regulated by extracellular antagonists, such as sclerostin, a secreted glycoprotein primarily produced by osteocytes. Acting as a negative regulator, it binds to the low-density lipoprotein receptor-related proteins (LRP5/6) coreceptors, leading to phosphorylation and degradation of  $\beta$ -catenin, thereby suppressing osteoblast maturation and new bone formation<sup>3,4</sup>. Osteocytes, by secreting sclerostin, play a central role in signaling the termination of the remodeling phase. Structurally, sclerostin consists of 213 amino acids and has a molecular weight of 22-24 kDa. It belongs to the bone morphogenetic protein (BMP) antagonist family and is encoded on chromosome 17 within the 17q12-q21 region by the SOST gene<sup>5-8</sup>.

Although sclerostin is most abundant in bone, it can be found in cartilage, kidney, liver, pancreas, heart, and plasma. While its exact function in these tissues has not yet been fully understood, it is believed to regulate the activity of bone-forming and bone-resorbing cells, maintaining bone homeostasis<sup>9,10</sup>. It acts as a potent anti-anabolic factor with its expression modulated by mechanical loading and cytokine signaling in bone tissue, ultimately determining the sclerostin levels in bones<sup>8-10</sup>. Winkler et al. first discovered sclerostin in adult human osteocytes. Elevated sclerostin levels inhibit osteoblastogenesis which is the formation of new bone tissue, and reduce bone formation, whereas downregulation of sclerostin expression enhances bone mass<sup>1,7,11-13</sup>.

Targeting sclerostin with neutralizing antibodies has therefore emerged as an attractive therapeutic approach for skeletal regeneration. Disruption of the interaction between the LRP5/6 and sclerostin is essential for Wnt-related metabolic processes that can affect

bone health. Consequently, in our previous study, we targeted the loop 2 region of sclerostin, which binds stably to LRP5/6, and employed a series of in silico approaches, including molecular docking and molecular dynamics simulations, to screen drug-like compounds from the Drug-Bank database<sup>14</sup>.

In recent years, significant research has been conducted on sclerostin, focusing on its administration both systemically and subcutaneously. While these studies have contributed valuable insights into its therapeutic potential, further investigation is still needed to fully understand its applications. One promising area of study is the potential use of sclerostin antagonists (romosozumab, blosozumab and bps804) to promote bone formation and treat osteoporosis<sup>15</sup>. Furthermore, the rare high bone mass disorder sclerosteosis and Van Buchen disease are known to be associated with beta-catenin-dependent Wnt signaling, which is linked to loss-of-function mutations of SOST. The cellular and molecular mechanisms of glucocorticoid-induced osteoporosis involve the suppression of Wnt signaling, resulting in the inhibition of osteoblast differentiation. Additionally, during immobilization-induced osteoporosis, sclerostin concentrations led to increased inhibition of bone formation.

In addition, experimental studies have provided compelling evidence of sclerostin inhibition in bone repair. For example, Nakashima et al. 2024 demonstrated that enhanced bone formation and wound healing were observed in the tooth extraction socket via a study model of bisphosphonate-induced osteonecrosis of the jaw (ONJ) model in combination with severe periodontitis to evaluate the development of ONJ and bone formation in wild-type (WT) and sclerostin knockout mice<sup>16</sup>. Periodontitis permanently damages the soft tissue and alveolar bone, resulting in tooth mobility and, ultimately, tooth loss. This irreversible cascade of bone loss in periodontitis needs therapeutic interventions. A recent study by Nascimento et al. 2024 ranked periodontitis as the sixthmost prevalent health condition globally, and in 2024, the Bangkok Declaration motto was No Health Without Oral Health<sup>17</sup>.

Therefore, the rationale of this study was to investigate the therapeutic potential of sclerostin inhibition for bone regeneration following tooth extraction. Specifically, we aimed to determine whether local, single-dose administration of a sclerostin-neutralizing antibody (Scl-ab) combined with a bone graft could enhance bone formation by curtailing

bone resorption. The primary objective was to evaluate the efficacy of targeted sclerostin inhibition in accelerating early socket healing and improving bone quality in a rabbit model.

# **MATERIALS AND METHODS**

# Experimental animal preparation, extraction of teeth, and treatment protocols

The male New Zealand albino rabbits, approximately three months old and weighing 2.5-3 kg, were used for physiological consistency and allowed to acclimate to their environment for several days before undergoing anesthesia to ensure their comfort. They were individually housed in cages equipped with environmental controls to maintain a stable temperature and humidity and were provided with a standard diet and water that was always available. After completing and practicing the preliminary research, extracting the first premolars proved to be the most effective course of action. The rabbits were randomly assigned to the three experimental and two control groups to eliminate any potential bias that could affect the results. Briefly, in the first place, all animals were anesthetized using xylazine HCl (5 mg/kg, i.m.) and ketamine (35 mg/kg, i.m.) followed by applying a customized mouth opener to hold the rabbit's mouth open (Utility Model Patent 2021-008511 as "Auxiliary Oral Support For Veterinary Applications). Thereafter, a standard experimental design was employed for tooth extraction, as detailed in Ergünol et al. (2025). Extraction of the right and left premolar teeth for two consecutive weeks would be four weeks of healing for the right and 2 weeks for the left.

After the premolar tooth extraction, the alveolar sockets underwent our treatment protocol. The extraction areas were filled with graft material (Cerabone Granulate, grain size 0.5-1.0mm, Straumann, Botis Biomaterials, Ref No: BO1515, GmbH) and graft material mixed with sclerostin-ab (Scl-ab, abcam 63097). The socket entry was sutured, and the animals were sacrificed after a two-week wait from the last extraction. Groups were the control (Group 1, only tooth extraction, physiological healing), graft used group (Group 2, 50 mg graft material), and the experimental groups as Group 3, Scl-ab (%100), 0.02 mg Scl-ab in 50 mg graft material, Group 4, Scl-ab (%75), and Group 5, Scl-ab (%50), in 50 mg graft material.

### Radiologic analysis

The present study utilized the HDX WILL DENTRI 3D cone beam computed tomography (CBCT) device manufactured by HDX WILL Corp. in Korea for irradiation. The CBCT device was used to cover a specific area of the field of view (FOV), measuring 160 x 80 mm. To ensure the unbiasedness of the results, a single technician made the dose adjustments. After irradiation, the images were reconstructed using specific parameters, such as 80-100 kV, 4-10 mA, a 200 µm voxel size, and an 8-24 second acquisition time. The images were then analyzed and measured by a single operator on axial, sagittal, frontal, and cross-sectional sections utilizing the Cybermed On-demand software from Cybermed Inc. in Korea. The images were further processed using CS 3D imaging software developed by Carestream Health Inc. in Rochester, NY, USA. The volumetric measurements were performed after selecting a standardized region of interest consisting of alveolar bone surrounding the socket area of the premolar tooth. The analyzed region was defined as the area between the alveolar crest and the apex of the teeth, standardized to 24.63 mm<sup>2</sup> for each specimen, serving as the region of interest (Figure 1). A single investigator plotted the periphery of the desired region of alveolar bone on 2D parasagittal images to maximize the amount of bone formed and minimize the inclusion of cavities. The bone volume per total volume, trabecular thickness and trabecular separation were then calculated from each specimen. To implement a novel automated enclosing convex polygon method, the Density distribution BoneJ ImageJ plug-in was modified. This application has multiple steps to specify cortical results, mass and density distribution, and concentric density distribution<sup>19-22</sup>.

# Histological analysis

The tissue samples of the whole mandible underwent a meticulous preparation process to guarantee precision during analysis. Initially, they were immersed in a 10% neutral formaldehyde solution with a pH of 7.3 for 24 hours to fix and preserve their structure. The decalcification process was achieved using EDTA at a pH of 7.4 to eliminate any calcium deposits that could interfere with the analysis<sup>23</sup>. After fixation and decalcification, the tissues were thoroughly washed with water and subjected to 70%, 80%, and 96% ethyl alcohol washes for 20 minutes each. This step was crucial in removing any residual

formaldehyde and EDTA that could impact the analysis. The tissues were washed with acetone in four rounds of 20 minutes each to eradicate residual water and alcohol.

Next, the tissues were submerged in Xylene I and Xylol II for 30 minutes each to eliminate any remaining traces of acetone. Once thoroughly cleaned, the tissues were placed in Paraffin I and Paraffin II and melted at 60°C for an hour. This step enabled the tissues to be embedded in paraffin blocks, and sections of 6 µm thickness were produced using a microtome. Finally, the hematoxylin-eosin procedure was employed to examine the general histomorphology of the sections, which were then studied under light microscopy. To ensure precise results, each section was thoroughly analyzed using an advanced PC-based image analysis system (Leica Qwin, Leica Ltd., Germany).

#### **Ethical statement**

All the animal experiments were conducted in accordance with the Guidelines for the Care and Use of

Laboratory Animals that were established, reviewed, and approved by the Local Ethics Committee for Animal Experiments at the University of Gazi (G.Ü.ET-20.007). The experimental procedure mostly complied with the Animal Research: Reporting of *in vivo* Experiments (ARRIVE) guidelines to ensure ethical, transparent, and reproducible animal research.

## Statistical analysis

All statistical analyses were conducted using SPSS software for Windows, version 18.0 (SPSS Inc., Chicago, IL, USA). Descriptive statistics are presented as means ± standard deviations (SD), with a significance level set at 5% (p < 0.05) for all tests. The distribution of the data was assessed using the Shapiro–Wilk test and visually confirmed with box plots. The homogeneity of variances was examined with Levene's test, which ensured the validity of parametric analyses. Subgroup analyses were carried out based on experimental weeks, comparing the control, graft, and sclerostin (Scl) groups separately. A mixed-design analysis of variance (mixed ANOVA) was performed to evaluate both within-group (time) and between-group effects on bone density. When significant main or interaction effects were found, a post hoc test was applied for pairwise comparisons, with corrections for multiple comparisons to control the type I error rate. Post hoc results

were reported with 95% confidence intervals (CIs), including both lower and upper bounds of the mean differences. When the assumptions for parametric testing were not met, non-parametric alternatives were used. Specifically, Wilcoxon signed-rank tests were conducted for paired comparisons where appropriate. To ensure the robustness of the study design, a post-hoc power analysis was performed to assess whether the sample size provided sufficient statistical power (>80%) to detect meaningful differences across groups and time points. Effect sizes (Cohen's d or partial eta squared, depending on the test) were also calculated to complement p-values, quantifying the magnitude of observed effects.

#### RESULTS

This experimental research entailed a meticulous and extensive analysis of the impact of sclerostin-ab (Scl-ab) treatment on alveolar bone formation. To achieve this, we conducted a detailed investigation to examine the inhibitory effect of sclerostin on bone formation during local administration. Using CBCT scans, various aspects of mandibular bone volume in a rabbit model were measured with a single dose of a locally administered Scl-ab and graft material combination for 2 and 4 weeks.

Five animals were used for each group in the study. Since sockets were obtained from the same rabbits at both 2 and 4 weeks, it was considered that the assumption of independent samples might be partially violated. Therefore, the unit of analysis was "animal," not "socket," and statistics were conducted using mean values per animal. Mixed-designed ANOVA revealed significant differences between the groups (F(4,20) = 2.074.938, p < 0.0001). Effect size calculations indicated a highly significant effect size with  $\eta^2 = 0.9999$  and Cohen's  $f \approx 644$ .

A post-hoc power analysis was conducted considering the observed variance and sample size, and  $1-\beta=1.0$  was found. This result shows that the statistical power of the study is at the maximum level, and therefore, the differences obtained are not due to insufficient sampling and are strongly supported.

The selected 3D images, obtained from cone-beam computed tomography (CBCT) results, are illustrated in Figure 2. All groups' right sagittal views represent two weeks, and the left sagittal views represent 4 weeks of treatment.

Figure 2-A1 depicts the control group. When the negligible tooth remnant is omitted, the empty socket area displays hypodensity with minimal bone regeneration. The empty socket areas showed no signs of new bone formation, resulting in a predominantly empty defect. By the 4-week mark, the same trends persisted, with the alveolar space remaining hypodense and largely empty. Figure 2-B1 represents the graft group. This image demonstrates a grafting procedure applied to the first premolar on both sides. The graft group displayed notable advancements in bone healing by week 2. In the right coronal view, a hypodense area measuring 5.79 mm, representing the alveolar space, is contrasted with a hyperdense area of 5.56 mm corresponding to the graft material. The left coronal view shows that the entire socket is filled with the graft material and appears hyperdense. In the left sagittal view, a hyperdense region corresponding to the graft material measures 3.37 x 9.22 mm. By week 4, there was a significant increase in both the volume and density of the socket. The left coronal view demonstrated that the entire socket was filled with graft material, appearing hyperdense. Figure 2-C1 displays the results for Scl-abfilled tooth sockets on both sides of the first premolars. The right coronal view demonstrates an alveolar space of 1.85 mm and a solid region of 8.29 mm, nearly filling the socket. The right sagittal view reveals a dense area covering most of the socket. In the left coronal view, a dense area of approximately 6.27 mm is observed between two empty regions measuring 2.63 mm and 1.78 mm, respectively. The left socket contains less filling material compared to the right socket. Figure 2-D1 presents the right sagittal image, where a dense material approximately 7.32 mm in length is observed, nearly filling the socket. Additionally, a less dense alveolar space measuring 1.73 mm is noted. The left sagittal image reveals a dense material of 4.29 mm and a less dense area of 2.27 mm within the alveolar space. Figure 2-E1 shows the Scl-ab-filled socket with 50% of the total material, as depicted in the right sagittal image, a hyperdense concretion measuring 7.7 mm, and a slightly hypodense socket cavity of 3.5 mm. A hyperdense tooth fracture approximately 5.02 mm in length is seen in the left sagittal image. The coronal and axial images corroborate these findings, with no evidence of material flare observed.

According to the Levene test results, variance homogeneity was achieved between the groups in the 2nd week measurements for the BV/TV parameter, and the variances were found to be similar (F (4, 20) = 1.294, p = 0.306). However, the variance distribution was not homogeneous in the 4th week, and a significant difference was observed between the groups (F (4, 20) = 16.668, p < 0.0001). When evaluated in terms of Tb.Th., variance homogeneity was not achieved between the groups, both in the 2nd week (F (4, 20) = 2.992, p = 0.044) and in the 4th week (F (4, 20) = 3.400, p = 0.028). When Tb.Sp. measurements were examined, the variances were found to be homogeneous in the 2nd week (F (4, 20) = 1.635, p = 0.205), but in the 4th week, the assumption of homogeneity was broken, and a significant difference was found between the groups (F(4, 20) =19.254, p < 0.0001). To strengthen the manuscript, the primary endpoints were reanalyzed using a Robust method. Robust tests (Welch's ANOVA and Brown–Forsythe) were conducted to evaluate group differences for bone morphometric parameters, as the assumption of homogeneity of variances was not fully met. The analyses revealed statistically significant differences among groups for all variables except for the 4th week for Tb.Sp. For BV/TV, Welch's test indicated a significant group effect, F(4, 9.54) = 164.69, p < 0.001, and this was confirmed by the Brown-Forsythe test, F(4, 12.40) =130.77, p < 0.001. For 4th week BV/TV, Welch's test yielded F(4, 9.01) = 596.03, p < 0.001 and Brown–Forsythe showed F(4, 9.52) = 135.60, p < 0.001.

For 2nd week Tb.Th. Welch's test was significant, F(4, 9.23) = 64.35, p < 0.001, as was Brown–Forsythe, F(4,13.73) = 48.08, p < 0.001. Similarly, for 4th week Tb.Th., Welch's test showed F(4, 8.09) = 82.75, p < 0.001, and Brown–Forsythe yielded F(4, 12.66) = 54.56, p < 0.001. For 2nd week Tb.Sp. Welch's test was significant, F(4, 8.05) = 59.93, p < 0.001, and Brown–Forsythe confirmed this, F(4, 14.10) = 30.68, p < 0.001. However, For 4th week Tb.Sp. robust tests could not be performed because at least one group had zero variance, which precluded the computation of the test statistics.

Besides, the results of Mauchly's sphericity test showed that the sphericity assumption was met for all parameters (BV/TV, Tb.Th. and Tb. Sp.) (W=1.000,  $\chi^2$ =0.000, p=1.000); therefore, no sphericity correction was required.

Taking into account the tests of within-subjects effects, the linear time effect statistical analyses showed that time had a significant effect on the BV/TV parameter (F(1, N) = 71.814, p < 0.001, partial  $\eta^2 = 0.782$ ). However, the time × group interaction was not significant for the linear contrast (F(4, N) = 2.083, p = 0.121, partial  $\eta^2 = 0.294$ ). These findings reveal that BV/TV values showed a significant change over time; however, this change followed a similar course across groups, with no group changing faster or slower than the others.

The linear time effect was found to be statistically significant for the Tb.Th. parameter  $(F(1, df) = 41.354, p < 0.001, partial <math>\eta^2 = 0.674)$ , and the time factor alone caused a strong change in the measurements. On the other hand, the time × group interaction was significant in terms of linear contrast  $(F(4, df) = 7.696, p = 0.001, partial \eta^2 = 0.606)$ , indicating that changes in trabecular thickness did not occur at the same level in all groups, with significant increases observed in some groups, while more limited changes occurred in others. Similarly, the Tb.Sp. parameter also showed significant differences over the linear effect of time  $(F(1, df) = 13.894, p = 0.001, partial \eta^2 = 0.410)$ , indicating that time alone strongly affected the measurements. In addition, the time × group interaction was found to be quite strong and significant in terms of linear contrast  $(F(4, df) = 51.082, p < 0.0001, partial \eta^2 = 0.911)$ , which reveals that the Tb. Sp changes of different groups over time were significantly different from one another.

Since the time x group interaction for BV/TV was not significant, no Wilcoxon test or other testing was necessary. This indicates that the groups did not change differently over time. There was no difference between the groups over time. Multiple comparison corrections were used for p-values in the comparisons made between Tb. Th. and Tb. Sp. After the Bonferroni correction, corrected p-values were calculated for both parameters, and no comparison was found to be statistically significant (p>0.05). In the evaluation performed with the Holm correction, p-values were calculated for both parameters; however, this method also failed to achieve statistical significance (p > 0.05). Therefore, even values that initially appeared close to significance were not found to be statistically significant in the comparisons between weeks 2 and 4 after multiple testing correction.

The control and graft groups exhibit minimal changes in BV/TV over time, with values significantly lower than those of experimental treatment groups. Sclerostin-ab significantly increases bone volume fraction (BV/TV), with the most pronounced effect observed at the 100% dose.

In the results observed over four weeks, the Scl-Ab 100% group demonstrated the highest at  $0.730 \pm 0.010$ , exhibiting a statistically significant difference compared to the control group (p=0.0001). The Scl-Ab 75% group showed a BV/TV of  $0.648 \pm 0.035$ , while the Scl-Ab 50% group displayed a BV/TV of  $0.588 \pm 0.039$ , both of which also indicated significant increases in bone volume (p=0.002, p=0.022, respectively) compared to the control group.

On the other hand, the graft group recorded a BV/TV of  $0.402 \pm 0.013$  (4 weeks) and  $0.356 \pm 0.012$  (2 weeks) lower than the control group's BV/TV of  $0.489 \pm 0.005$  (p = 0.0001) and 45.97 0.89 (p = 0.0001), respectively (Figure 3 and Table 1, Table 4 and Table 5).

Between-group effect analysis showed that the intercept effect was significant for the BV/TV parameter (F(1, df) = 29831.770, p<0.0001, partial  $\eta^2$  = 0.999). Also, quite strong and significant differences were found between the groups in terms of BV/TV values (F(4, df) = 294.578, p<0.0001, partial  $\eta^2$  = 0.983). The effect size of the group effect is quite high ( $\eta^2$ p=0.983) and this result shows that more than 98% of the BV/TV variance is explained by the group factor. Similarly, the intercept effect was also significant for the Tb.Th. value (F(1, df) = 25788.769, p < 0.0001, partial  $\eta^2$  = 0.999) and strong differences were observed between the groups (F(4, df) = 84.457, p < 0.0001, partial  $\eta^2$  = 0.944). The effect size obtained ( $\eta^2$ p=0.944) reveals that the group factor has a strong effect on Tb.Th. and explains approximately 94% of the variance.

In the analysis conducted for the Tb.Sp. parameter, the intercept effect was found to be significant (F(1, df) = 9139.569, p< 0.0001, partial  $\eta^2$  = 0.998) and statistically significant differences were found between the groups (F(4, df) = 157.851, p<0.0001, partial  $\eta^2$  = 0.969). The group effect was found to be at a very high level ( $\eta^2$ p=0.969), and this result shows that 97% of the variance in Tb.Sp. values — are due to the group factor. These findings reveal that the different groups applied to all the BV/TV, Tb. Th., and Tb.Sp. values produced significant and strong effects (Table 3).

The data assessment was continued with a multiple comparison evaluation, which revealed significant differences between the groups regarding the BV/TV, trabecular thickness (Tb.Th), and trabecular separation (Tb. Sp.) values at two and four weeks.

During 2-week period the control and graft group showed significantly lower BV/TV values compared to the Scl-ab 100% (p=0.0001), Scl-ab 75% (p=0.0001) and Scl-ab 50% group (p=0.001, p=0.0001, respectively). The Scl-ab 100% group achieved the highest BV/TV ratio among all groups and provided a statistically significant increase compared to the control, Scl-ab 75%, and Scl-ab 50% (p=0.0001 for all comparisons) groups. The Scl-ab 75% group exhibited significantly higher BV/TV values than the control and graft (p=0.0001 for both) groups, but was found to be significantly lower compared to the Scl-ab 100% group (p=0.0001), and no difference was observed for the Scl-ab 50% group (p=0.108). The Scl-ab 50% group showed a significant increase compared to the graft group (p=0.0001) and also exhibited higher values compared to the control group (p=0.001) (Table 1, Table 4).

After 4 weeks of treatment, the BV/TV values of Scl-ab 75% group were significantly lower than the Scl-ab 100% group (p=0.024). The difference between this group and the Scl-ab 50% group was not statistically significant (p=0.175). The Scl-Ab 50% group showed a significantly higher BV/TV ratio than the graft group (p=0.001) and was also significantly higher than the control group (p=0.022). However, it showed lower values than the Scl-Ab 100% group (p=0.005), and no significant difference was found with the Scl-Ab 75% group (p=0.175) (Table 1, Table 5)

This dosage results in the most significant enhancement over time. Although the 75% and 50% doses of sclerostin-ab also promote increased bone volume, their impacts are less substantial, highlighting a clear dose-dependent response. Specifically, the Scl-Ab 100% group achieved the highest BV/TV ratio, providing the strongest effect, while the graft group maintained the lowest values, providing a limited contribution to bone volume

The second value for the region of interest was the alveolar bone's trabecular thickness (Tb.Th.) that revealed a significant enhancement following Scl-ab administration for 2 and 4 weeks. Compared to the control group of 2 weeks, which presented a Tb.Th. of

 $0.148 \pm 0.002$  mm, the graft group displayed a reduced Tb.Th. of  $0.121 \pm 0.009$  mm (p=0.009). The Scl-ab 100% group achieved the highest Tb.Th. as 0.176±0.004 mm compared to the control and graft groups for 2 weeks (p=0.0001 for both). Furthermore, the Scl-ab 75% and 50% groups also demonstrated increases in Tb.Th. with measurements of  $0.168 \pm 0.008$  mm, which is significant (p=0.022), and  $0.158 \pm 0.008$ mm, not significant (p=0.209), respectively, compared to the control group. Both Scl-ab 75% and 50% demonstrated significant increases in Tb.Th. compared to the graft group (p=0.0001, p=0.001, respectively). Although having higher Tb.Th. values compared to control and graft group (p=0.022, p=0.0001, respectively) the Scl-ab 75% group exhibited no differences to Scl-ab 100% and 50% groups (p=0.425, p=0.392, respectively). The Scl-ab 50% group showed a significant increase compared to the graft group (p=0.001), and the differences were not statistically significant compared to the control and Scl-ab 75% groups. In addition, the graft group exhibited the lowest Tb.Th values compared to all groups (p<0.05) (Table 1, Table 6).

After the 4 weeks of treatment, the Scl-Ab 100% group exhibited the highest Tb.Th. of  $0.196 \pm 0.004$  mm compared to the control and graft groups (p=0.0001, for both). The Scl-Ab 75% group was not statistically different (p=0.291) from the control group with measurements of  $0.172 \pm 0.008$  mm, but different from the graft group (p=0.001). Also, Scl-ab 50% group values were not different than  $(0.154 \pm 0.009$  mm) the control group (p=0.305) and the graft group (p=0.136), only recorded significantly lower Tb.Th. values compared to the Scl-ab 100% group (p=0.001). The graft group again had the lowest Tb.Th values, which were significantly lower than the control group (p=0.004) and not different from the Scl-ab 50% group (p=0.136). (Table 1, Table 6).

For the 2 weeks, only the comparison between Scl-ab 100% and Scl-ab 75% Tb.Th. was not significantly different (p=0.425). But after 4 weeks, all doses were statistically significantly different (p<0.05, Table 6).

It was clearly demonstrated that the graft group exhibited the lowest Tb.Th. values at both time points, while the Scl-ab 100% group reached the highest values (Table1).

Furthermore, it can be reported that the effect of the Scl-Ab 100% application became more pronounced over time, while the Scl-ab 75% and 50% groups exhibited values close to the control level. These results suggest that Scl-ab application exhibits a dose-dependent effect, and that the 100% application, in particular, plays a strong role in improving trabecular thickness.

Regarding the multiple comparisons of Tb.Sp values for the two-week duration, compared to the control group, which demonstrated a trabecular separation (Tb.Sp) of  $0.0699 \pm 0.0003$  mm, the graft group showed a Tb.Sp of  $0.0439 \pm 0.0042$  mm (p = 0.0001). Scl-ab 100% exhibited a similar Tb.Sp. of  $0.0696 \pm 0.0055$  mm compared to the control group (p>0.05). However, the Scl-ab 75% group showed a significant reduction, measuring  $0.0600 \pm 0.0070$  mm compared to the control group (p=0.039) but higher than the graft group (p=0.001). Scl-ab 50% group had a value of  $0.046 \pm 0.0055$  mm Tb.Sp. that was significantly lower than the control group (p=0.0001) but similar to the graft group (p=0.962) (Table 1, Table 7).

The Tb. Sp. evaluation showed that the control and Scl-ab 100% groups exhibited the highest trabecular thickness of the marrow cavities structure. The graft and Scl-Ab 50% groups exhibited the weakest trabecular structure, and the Scl-Ab 75% group showed a significantly closer Tb.Sp. results to control and Scl-ab 100%.

During the four-week evaluation, it was determined that the control group (0.0840 ± 0.0001 mm) had significantly higher Tb.Sp values compared to the graft (p=0.0001), Scl-ab 100% (p=0.024). Scl-ab 75% (p=0.0001) and Scl-ab 50% (p=0.0001) groups. The graft group (0.0500 ± 0.0001) showed a higher Tb.Sp values compared to Scl-ab 75% (p=0.0001) and 50% (p=0.0001), and significantly lower than the Scl-ab 100% (p=0.005) and control group (p=0.0001). The Scl-ab 100% group (0.0704±0.0055 mm) Tb.Sp. values were significantly higher than the graft (p=0.005), Scl-ab 75% (p=0.0001), and Scl-ab 50% (p=0.001) groups, and were significantly lower than the control group (p=0.24). The Scl-Ab 75% group showed significantly lower Tb.Sp. values compared to the control, graft, and Scl-Ab 100% groups (p=0.0001 for all), and was found to be similar to the Scl-ab 50% group. Similarly, the Scl-ab 50% group had

significantly lower Tb.Sp. values compared to the control, graft, and Scl-ab 100% groups (p<0.001 for all) (Table 8).

These results show that the control group exhibited the weakest trabecular structure, characterized by the highest Tb.Sp. values over the four-week period, while the Sclab 75% and 50% groups exhibited the tightest trabecular structure with the lowest Tb.Sp values. Further, the Sclab 100% application in the early period (week 2) had the same trabecular spaces as in the control group, but this effect decreased in the later period (week 4), and the positive effects of Sclab 75% and 50% applications became evident over time (Tables 7 and 8).

# **Histological results**

The histological observations are depicted in Figure 4. It provides a basis for identifying potential changes when comparing the control group to the graft and experimental groups. This comparison was crucial in determining any deviations in tissue response and healing patterns between the control and treated groups, providing insights into the effects of the various interventions on tissue regeneration and bone formation. To thoroughly assess the outcomes, we conducted a detailed histological analysis to identify group differences. The hematoxylin and eosin (H&E) staining was used as a standard technique outlined in the materials and methods section under histological analysis.

Additionally, both groups that received the graft after 2 and 4 weeks demonstrated lower levels of vascularization and regular bone formation compared to the Scl-Ab groups. However, after four weeks, the group that received the graft exhibited more advanced bone growth than the group after two weeks, as evident in Figures 4c and 4d. In Group 3, which received graft and Scl-ab 100%, notably increased vascularization was observed in the 2 and 4-week groups. Unlike in the graft group, the new capillary formation did not regress in these groups. Furthermore, the number of inflammatory cells increased significantly. The newly formed bone tissue looked the most mature and had the highest amount of newly formed bone trabeculae in the Scl-ab 100% of 2 and 4-week groups, respectively. Upon further analysis, the Scl-ab 100% 2-week group demonstrated a significant increase in osteoblasts. This is supported by the data presented in Figure 4(e).

Besides, capillarization was more pronounced in the Scl-ab 100% 4-week group, as shown in Figure 4(f). A well-developed vascular network was observed in Group 4, which received a combination of Graft and 75% Scl-ab. The degree of capillarization was notably higher than that observed at the 2-week interval (Figure 4g and 4h). In Group 5, graft and 50% Scl-ab, the histological analysis revealed a favourable outcome regarding connective tissue density and bone formation.

#### DISCUSSION

Our group conducted a comprehensive study to assess the effects of locally administering sclerostin antibody (Scl-ab) on bone formation after tooth extraction and grafting. The strength of this research is its focus on the therapeutic potential of Scl-ab to enhance bone regeneration and improve the quality of bone in extraction sockets. Different bone loss or bone injury settings, such as the femoral or alveolar defect models, were preclinically investigated. However, those models were not directly extrapolatable to the clinical condition of teeth extraction models. The jawbones differ in characteristics because the origin of bone tissues differed<sup>24,25</sup>.

The primary objective of our research was to investigate the effect of Scl-ab on bone formation using graft materials in tooth sockets. To examine the impact of Scl-ab, after completing CBCT analysis of the mandibles, the region of interest was determined for the volumetric analysis, and enhanced bone regeneration in the mandibular region was observed.

Our analysis revealed that the tooth extraction sockets treated with various ratios of Sclab with graft material showed a statistically significant increase in the mean mandibular BV/TV ratio compared to the control and graft groups (Figure 3 and Table 1), depending on time and dosage. While bone volume shows improvement over time, the most remarkable increase is evident in the 100% Scl-ab group. The administration of various doses of Scl-ab also significantly increased trabecular thickness of alveolar bone, which is the average thickness of all bone voxels<sup>26</sup>, a vital indicator of bone quality, microstructure, and formation in a clinical setting, compared to control (p<0.001) and graft (p<0.001) groups, where histological analysis supported all data. However, no

differences were observed between the 4-week treatment groups of Scl-ab 50% and the control and graft groups, and between Scl-ab 75% and the control and Scl-ab 50% groups (p > 0.05).

This increase was consistent across the 2-week and 4-week treatment periods, indicating a positive effect of Scl-Ab on mandibular bone formation. Results suggest that Scl-ab contributes to overall bone volume and enhances the structural integrity of the trabecular network within the alveolar bone, with its efficacy closely linked to the administered dose. After 4 weeks, the trabecular separation (Tb.Sp), which is the thickness of the marrow cavities, was lower than that of the control group. It is important to note that new bone formation increases, and the trabecular structure becomes denser. In particular, Scl-Ab treatment is thought to positively affect trabecular bone microarchitecture, reduce intrabone spaces, and facilitate the integration of new bone tissue. This clearly demonstrates the osteogenic effects of sclerostin inhibitors and their potential role in bone regeneration. As a result, the decrease in Tb.Sp. values observed in the study indicate that the application of Scl-ab particularly supports early bone healing and enhances trabecular architecture. This finding reinforces the potential use of sclerostin inhibitors as biological agents in regenerative therapies.

Although reliable statistical tests (Welch ANOVA and Brown-Forsythe) showed significant differences between experimental groups' data for 2 and 4 weeks of BV/TV, Tb.Th, and only for 2 weeks of Tb.Sp. (p < 0.001), results demonstrated distinct group-dependent changes in trabecular bone volume and microarchitectural organization, with a limitation of robust tests for 4-week Tb.Sp. data that could not be performed due to zero variance in at least one group, precluding reliable statistical estimation. Another limitation could be that measurements were performed by a single experienced operator, which may have reduced variability; however, no formal intra-observer ICC analysis was conducted.

Researchers have employed various animal models to gain insights into the complex workings of the Wnt/β-catenin pathway, including knockout, transgenic, and overexpressing models. These models have proven invaluable in unravelling the complex interplay between this pathway, the frizzled receptors, and LRP5/6 on the cell membrane<sup>3,27</sup>. Additionally, the Wnt pathway has been implicated in the homeostatic

regulation of the periodontal ligament and alveolar bone. It has been shown to mediate force-induced bone modeling during orthodontic tooth movement. In their study, Disha-İbrahimi et al. suggested that during force bone modeling, the downregulation of gene expression levels of the Wnt/beta-catenin signaling pathway directs target genes, and osteocyte maturation is related to the treatment<sup>28</sup>. In their current study, Turkkahraman et al. investigated the effects of Scl-Ab on craniofacial tissues in a healthy and adult-onset mouse model of established type 2 diabetes (T2D), demonstrating severe alveolar bone loss and periodontal soft tissue degeneration, which mimics the periodontal disease exhibited by patients with T2D. Systemic treatment with Scl-ab increased the alveolar bone volume, reversed the effects of T2D on remodeling by increasing osteogenic cells and decreasing osteoclasts, and rescued the bone loss. Remarkably, the Scl-Ab treatment also had protective effects on the periodontal soft tissues, promoting the proliferation of disintegrated periodontal ligament cells, increasing collagen fiber density, preserving extracellular matrix expression, and reducing inflammation<sup>29</sup>. Taut et al. also showed that systemic Scl-ab applied to rats with experimental periodontitis improved alveolar bone mass<sup>30</sup>. In a different study, Yao et al. created alveolar bone defects in rats and investigated the use of systemically-delivered versus low-dose locally-delivered Scl-ab via polylactic-co-glycolic acid microspheres (MSs) and concluded that systemic Scl-ab administration improved bone regeneration and tended to increase cementogenesis measured by histology and microcomputed tomography<sup>31</sup> and no studies had evaluated Scl-ab to repair osseous defects around teeth or to identify the efficacy of locally delivered Scl-ab for targeted drug delivery.

Bone loss cannot be fully reversed or stimulated to regrow using current methods. By focusing on the local administration of Scl-ab, our study aims to minimize systemic effects, thereby enhancing its potential for clinical application and yielding promising results.

The unique function of bone grafts is to provide mechanical support and stimulate osteogenesis for a bone replacement that needs the biological properties of osseointegration, osteogenesis, osteoconduction, and osteoinduction. They primarily serve as a structural framework to satisfy the osteoconductivity component of the ideal

characteristics<sup>32</sup>. Bone grafts are continually evolving to meet the needs of the patient population better. Some of the current needs include custom bone grafts for patients and synthetic grafts that replicate the qualities of autologous grafts. Alveolar bone grafting is a standard procedure in maxillofacial surgery that aims to reconstruct the alveolar ridge and provide a stable area for dental implants.

One of the challenges of this procedure is achieving successful osseointegration, which involves forming a direct structural and functional connection between the grafted bone and the surrounding tissues. In our graft-applied group, after four weeks, the level of capillarization, referring to the formation of small blood vessels, was low compared to 2 weeks. This reduction in capillary density over time suggests a potential decline in angiogenic activity. Vascularization was less pronounced in these graft-only groups, which may have impacted the efficiency of the healing process. In addition to reduced vascularization, these groups demonstrated less regular bone formation than the Scl-ab groups, indicating that the graft alone may not have provided the same support for consistent and structured bone regeneration.

Additionally, compared to control groups, the decline in BV/TV and Tb.Th. values were marked to indicate that while graft application alone cannot facilitate some degree of healing, vascular and bone formation may be more robust when additional factors, such as Scl-ab, are incorporated into the treatment regimen. This sustained capillary formation suggests a stable and ongoing angiogenic response, which is crucial for supporting the metabolic demands of the healing tissue. Contemporary bone grafting materials assist in regeneration but cannot wholly and efficiently mimic natural bone formation.

The histological examinations of the local/direct application of different doses of Scl-ab to the extraction sockets without bone defects to the alveolar bone triggered osteogenesis to a more regular and mature level, resulting in a notable increase in vascularization, newly formed bone tissue, and newly formed bone trabeculae. The positive effects of Scl-ab on the formation of new capillaries and the rise in the number of osteoblasts further support the potential of Scl-ab as an effective treatment for bone repair and regeneration.

The tissue exhibited a robust combination of our graft material with Scl-ab in a 2-week group, which showed a significant increase in osteoblast activity. Osteoblasts are the cells responsible for synthesizing new bone matrix, which were notably more abundant,

indicating an accelerated bone formation process. Moreover, capillarization was more pronounced in the Scl-ab 4-week groups, indicating a continued positive effect on new capillary formation. This enhanced capillarization is depicted in Figure 4f, further underscoring the efficacy of the 100% Scl-ab treatment in promoting both vascular and bone tissue regeneration. These findings collectively suggest that the combined application of graft and 100% Scl-ab support robust angiogenesis and enhance bone regeneration quality through increased osteoblast activity and sustained capillary development. In Group 4, which received a combination of graft and 75% Scl-Ab, the study demonstrated a well-developed vascular network indicative of effective angiogenesis within the treated area. The degree of capillarization—referring to the formation of new capillaries—was notably higher than that observed at the 2-week interval, suggesting a temporal improvement in vascularization as the healing process progressed.

Furthermore, the analysis revealed the presence of lamellation, a characteristic structural feature of mature bone, defined by its organized, layered matrix. However, a reduction in the extent of lamellation was observed, which could indicate an active phase of bone remodeling. The decrease in lamellar structure suggests that the bone is undergoing dynamic changes, likely involving the formation of new bone and the resorption of existing bone. This remodeling activity is crucial for adapting to mechanical stresses and maintaining bone integrity during the healing process. These findings are detailed in Figures 4g and 4h, underscoring the intricate balance between bone formation and remodeling within the combined graft and 75% Scl-Ab treatment. Also, in Group 5, the histological analysis revealed a favorable outcome regarding connective tissue density and bone formation matrix, indicative of effective graft integration and enhanced osteogenesis. Moreover, well-defined trabecular structures within the newly formed bone suggest active bone remodeling processes. Notably, the identification of multinucleated giant cells within the tissue further supports the occurrence of cellular responses associated with bone resorption and remodeling. These findings suggest that applying 50% Scl-ab in conjunction with the graft may enhance bone healing by promoting new bone formation and remodeling existing bone structures.

The osteoblast numbers were counted for all groups and were highest at week 4, compared to week 2, in the Scl-ab treated groups, suggesting that bone maturation was more advanced. The Scl-ab 100% group had the highest number of osteoblasts after 2 weeks (14), followed by the Scl-ab 75% (11), Scl-ab 50% (10), graft (9) and control (8) groups. At week 4, a decrease in the number of osteoblasts was observed in the Scl-ab 100% group (12) compared to week 2, where the numbers for Scl-ab 75% (13), Scl-ab 50% (13), graft (11), and 8 for the control groups. This suggests that osteoblasts may have shifted toward osteocytes in week 4, during the 4-week period which bone maturation is expected to progress in the most critical direction<sup>33,34</sup>.

Treatments targeting sclerostin may have therapeutic potential for bone-related disorders by promoting bone regeneration and enhancing bone quality in patients<sup>35</sup>. The anabolic response in the activity of Scl-ab that we observed in our research could be a significant breakthrough in treating bone-related ailments. Our findings provide valuable insights into the effectiveness of local Scl-ab use for bone growth and quality, as well as shortening the osseointegration period, which could pave the way for future clinical trials in this field. Both excess and deficiency of sclerostin significantly affect these factors. Long-term safety and efficacy studies will also increase the value of the results. We are optimistic that our research will contribute to the development of more effective treatments for bone loss and other skeletal conditions.

#### **CONCLUSION**

The local application of a therapeutic protein composition activates the bone healing process by turning local signaling mechanisms on and off, promoting efficient and natural-like bone healing. The inclusion of a sclerostin antibody stimulates efficient and natural-like bone formation, as demonstrated by histological analysis, which shows the development of vascularized bone tissue. This composition offers universal usability when combined with graft materials. Biocompatibility and straightforward application, enhancing adoption in clinical settings. This innovative approach significantly improves bone volume augmentation and overcomes the limitations of traditional bone grafting methods. It can also provide a game-changing strategy for dental professionals seeking faster recovery and superior long-term results.

Conflicts of interest: Authors declare no conflicts of interest.

**Funding:** This study was supported by the Gazi University Scientific Research Projects Coordination Unit (BAP) (project code: TCD-2021-7060).

**Data availability:** The materials described in the manuscript, including all relevant raw data, will be made available to any researcher wishing to use them for non-commercial purposes, provided participant confidentiality is not breached. Please get in touch with the corresponding author (asepicidincel@gmail.com) for further information.

Submitted: July 24, 2025

Accepted: October 14, 2025

Published online: October 22, 2025

#### REFERENCES

- 1. Winkler DG, Sutherland MK, Geoghegan JC, Yu C, Hayes T, Skonier JE, et al. Osteocyte control of bone formation via sclerostin, a novel BMP antagonist. EMBO J 2003;22:6267–6276. doi.org/10.1093/emboj/cdg599.
- 2. Lewiecki EM. Role of sclerostin in bone and cartilage and its potential as a therapeutic target in bone diseases. Ther Adv Musculoskelet Dis 2014;6(2):48–57. 10.1177/1759720x13510479
- 3. Gao Y, Chen N, Fu Z, Zhang Q. Progress of Wnt Signaling Pathway in Osteoporosis. Biomolecules 2023;13:483. doi.org/10.3390/biom13030483.
- 4. Semenov M, Tamai K, He X. SOST is a ligand for LRP5/LRP6 and a Wnt signaling inhibitor. J Biol Chem 2005;280(29):26770–5. doi.org/10.1074/jbc.M504308200.
- 5. Balemans W, Ebeling M, Patel N, Van Hul E, Olson P, Dioszegi M, et al. Increased bone density in sclerosteosis is due to the deficiency of a novel secreted protein (SOST). Hum. Mol. Genet 2011;10:537–544. 10.1093/hmg/10.5.537.
- 6. Van Hul W, Balemans W, Van Hul E, Dikkers FG, Obee H, Stokroos RJ, et al. Van Buchem disease (hyperostosis corticalis generalisata) maps to chromosome 17q12-q21. Am J Hum Genet 1998;62:391–399.
- 7. Winkler DG, Yu C, Geoghegan JC, Ojala EW, Skonier JE, Shpektor D, et al. Noggin and sclerostin bone morphogenetic protein antagonists form a mutually inhibitory complex. J Biol Chem 2004; 279:36293–8. 10.1074/jbc.M400521200.
- 8. Veverka V. Henry AJ, Slocombe PM, Ventom A, Mulloy B, Muskett FW, et al. Characterization of the structural features and interactions of sclerostin. J Biol Chem 2009;284:10890–10900. 10.1074/jbc.M807994200.
- 9. Delgado-Calle J, Sato AY, Bellido T. Role and mechanism of action of sclerostin in bone. J Bone 2017;96:29–37. 10.1016/j.bone.2016.10.007.
- 10. Weivoda MM, Youssef SJ, Jo Oursler M. Sclerostin expression and functions beyond the osteocyte. J Bone 2017;96:45–50. 10.1016/j.bone.2016.11.024 30.
- 11. Robling AG, Bellido T, Turner CH. Mechanical stimulation in vivo reduces osteocyte expression of sclerostin. Journal of Musculoskeletal & Deuronal Interactions 2006;6(4):35.

- 12. Ten Dijke P, Krause C, de Gorter DJ, Lowik CW, van Bezooijen RL. Osteocytederived sclerostin inhibits bone formation: its role in bone morphogenetic protein and Wnt signalling. J Bone Joint Surg Am 2008;90(1): 31.
- 13. Dincel AS, Jørgensen NR; IOF-IFCC Joint Committee on Bone Metabolism (C-BM). New emerging biomarkers for bone disease: Sclerostin and Dickkopf-1 (DKK1). Calcif Tissue Int 2023;112(2):243-257. doi.org/10.1007/s00223-022-01020-9.
- 14. Şimşek Y, Baran SS, Ergünol E, Uludamar A, Dinçel AS, Erkoç Ş. In silico identification of sclerostin inhibitors. Mol Divers 2025; Jul 29.doi:10.1007/s11030-025-11298-0. Epub ahead of print. PMID: 40728828.
- 15. do Amaral Couto BA, Fernandes JCH, Saavedra-Silva M, Hernan Roca H, Rogério Moraes Castilho MR, Fernandes GVO. Antisclerostin Effect on Osseointegration and Bone Remodeling J. Clin. Med. 2023, 12, 1294. doi.org/10.3390/jcm12041294
- 16. Nakashima F, Matsuda S, Ninomiya Y, Ueda T, Yasuda K, Hatano S, et al. Role of sclerostin deletion in bisphosphonate-induced osteonecrosis of the jaw. Bone 2024;187:117200.
- 17. Nascimento GG, Alves-Costa S, Romandini M. Burden of severe periodontitis and edentulism in 2021, with projections up to 2050: The Global Burden of Disease 2021 study. J Periodont Res. 2024; 59: 823-867. doi.org10.1111/jre.13337
- 18. Ergünol, E., Akgün, R.O., Şemsi, R., Ekim, O., Uludamar, A., and Dinçel, A.S. Novel Method for Tooth Extraction in Rabbits: Advantages and Considerations. Indian Journal of Animal Research 2025;1-6. doi:10.18805/IJAR.BF-1901 Epub ahead of print.
- 19. Dougherty R, Kunzelmann K. Computing local thickness of 3D structures with ImageJ. Microsc. Microanal. 2007;13:1678–1679. doi.org/10.1017/S1431927607074430 20. Doube M, Kłosowski MM, Arganda-Carreras I, Cordelières FP, Dougherty RP, Jackson JS, et al. BoneJ: Free and extensible bone image analysis in ImageJ. Bone. 2010 Dec;47(6):1076-9. doi.org/10.1016/j.bone.2010.08.023.
- 21. Recommended Citation: U.S. Food and Drug Administration. (2024). BoneJ Headless: An Automated Python Tool for Bone Microstructure Analysis (RST24AI03.01). <a href="https://cdrh-rst.fda.gov/bonej-headless-automated-python-tool-bone-microstructure-analysis">https://cdrh-rst.fda.gov/bonej-headless-automated-python-tool-bone-microstructure-analysis</a>

- 22. Ebrakhim, M.; Moiseev, D.; Strelnikov, V.; Salloum, A.; Faustova, E.; Ermolaev, A.; Enina, Y.; Velichko, E.; Vasil'ev, Y. A New Method for the Digital Assessment of the Relative Density of Bone Tissue in Dentistry Using the ImageJ Software Package. Dent. J. 2025, 13, 375. doi.org/10.3390/dj13080375
- 23. Sangeetha R, Uma K, Chandavarkar V. Comparison of routine decalcification methods with microwave decalcification of bone and teeth. J Oral Maxillofac Pathol 2013;17(3):386-91.
- 24. Sung HH, Kwon HH, Stephan C, Reynolds SM, Dai Z, Van der Kraan PM. Sclerostin antibody enhances implant osseointegration in bone with Col1a1 mutation. Bone 2024;186:117167.
- 25. Mavropoulos A, Rizzoli R, Ammann P. Different responsiveness of alveolar and tibial bone to bone loss stimuli, J. Bone Miner. Res. 2007;22: 403–410. [PubMed: 17181394]
- 26. Feng Zhu, Yong Qiu, Hiu Yan Yeung, Kwong Man Lee, Chun-yiu Jack Cheng. Trabecular bone micro-architecture and bone mineral density in adolescent idiopathic and congenital scoliosis. Orthopaedic Surgery 2009;1(1):78–83. doi.org/10.1111/j.1757-7861.2008.00014.x.
- 27. Marino S, et al. Reversal of the diabetic bone signature with anabolic therapies in mice. Bone Res. 2023;11(1):19.
- 28. Disha-Ibrahimi S, Furlani B, Drevenšek G, Hudoklin S, Marc J, Prodan Žitnik I, Sajovic J, Drevenšek M. Olanzapine decreased osteocyte maturation and Wnt/β-catenin signaling during loading of the alveolar bone in rats. Biomol Biomed 2023;1;23(1):114-125. doi.org.(10.17305/bjbms.2022.7523. PMID: 35880348; PMCID: PMC9901902.
- 29. Turkkahraman H, Flanagan S, Zhu T, Akel N, Marino S, Ortega-Gonzalez D, et al. Sclerostin antibody corrects periodontal disease in type 2 diabetic mice. JCI Insight 2024;9(16):e181940 doi.org/10.1172/jci.insight.181940.
- 30. Taut AD, Jin Q, Chung JH, Galindo-Moreno P, Yi ES, Sugai JV, Ke HZ, Liu M, Giannobile WV. Sclerostin antibody stimulates bone regeneration after experimental periodontitis. J Bone Miner Res 2013;28(11):2347-56. doi: 10.1002/jbmr.1984. PMID: 23712325

- 31. Yao Y, Kauffmann F, Maekawa S, Sarment LV, Sugai JV, Schmiedeler CA, Doherty EJ, Holdsworth G, Kostenuik PJ, Giannobile WV. Sclerostin antibody stimulates periodontal regeneration in large alveolar bone defects. Sci Rep 2020;1,10(1):16217. 10.1038/s41598-020-73026-y.
- 32. Zhao R, Yang R, Cooper PR, Khurshid Z, Shavandi A, Ratnayake J. Bone Grafts and Substitutes in Dentistry: A Review of Current Trends and Developments. Molecules 2021;18, 26(10):3007. doi: 10.3390/molecules26103007.
- 33. Kumala ELC, Fauzia M, Junivianti HS. The effect of nanoparticle tooth grafts on osteoblast stimulation in the first stages of the bone healing process in Wistar rats compared to the micro-tooth graft technique. Dental Journal 2023;56(3):184–188. doi.org/10.20473/j.djmkg.v56.i3.p184-188
- 34. Brannigan K, Griffin M. An update into the application of nanotechnology in bone healing. Open Orthop J 2016; 10(1): 808–23.
- 35. Choi RB, Bullock WA, Hoggatt AM, Loots GG, Genetos DC, Robling AG. Improving Bone Health by Optimizing the Anabolic Action of Wnt Inhibitor Multitargeting. JBMR Plus 2021;5(5):e10462. doi.org/: 10.1002/jbm4.10462.

# TABLES AND FIGURES WITH LEGENDS

Table 1. Tests of within-subjects effects

	Source		df	Mean square	F	Sig.	Partial Eta squared
BV/TV							
time	Sphericity assumed	.043	1	.043	71.814	0.001	.782
time x	Sphericity	.005	4	.001	2.083	0.121	.294
Groups	assumed						
Error (time)	Sphericity assumed	.012	20	.001			
Tb. Th.							
time	Sphericity assumed	.002	1	.002	41.354	0.001	.674
time x Groups	Sphericity assumed	.001	4	.000	7.696	0.001	.606
Error (time)	Sphericity assumed	.001	20	3.807E-5			
Tb. Sp.							
time	Sphericity assumed	.000	1	.000	13.894	0.001	.410
time x Groups	Sphericity assumed	.003	4	.001	51.082	0.001	.911

Error	Sphericity	.000	20	1.440E-5		
(time)	assumed					

Abbreviations: BV/TV: Bone volume/total volume; Tb.Th.: Trabecular thickness; Tb.Sp.: Trabecular separation; df: Degrees of freedom.

Table 2. CBCT bone morphometry by group at 2 and 4 weeks (n=5): BV/TV, Tb.Th., Tb.Sp. (mean  $\pm$  SD; 95% CI).

l p	Parameters			95% confiden	ce interval for
1	n=5		Std.	m€	ean
	n-3	Mean	deviation	Lower bound	Upper bound
BV/TV	Control	.4597	.00895	.4486	.4708
2 week	Graft	.3563	.01157	.3420	.3707
	Scl-Ab 100%	.6540	.02966	.6172	.6908
	Scl-Ab 75%	.5640	.01817	.5414	.5866
	Scl-Ab 50%	.5280	.03114	.4893	.5667
BV/TV	Control	.4884	.00477	.4825	.4943
4 week	Graft	.4020	.01304	.3858	.4182
	Scl-Ab 100%	.7300	.01000	.7176	.7424
	Scl-Ab 75%	.6480	.03493	.6046	.6914
	Scl-Ab 50%	.5880	.03962	.5388	.6372
Tb.Th.	Control	.1478	.00217	.1451	.1505
(mm)	Graft	.1207	.00894	.1096	.1318
2 week	Scl-Ab 100%	.1756	.00351	.1712	.1800
	Scl-Ab 75%	.1680	.00837	.1576	.1784
	Scl-Ab 50%	.1580	.00837	.1476	.1684
Tb.Th.	Control	.1632	.00045	.1626	.1638
(mm)	Graft	.1407	.00579	.1335	.1479

	Scl-Ab 100%	.1964	.00410	.1913	.2015
	Scl-Ab 75%	.1720	.00837	.1616	.1824
	Scl-Ab 50%	.1540	.00894	.1429	.1651
Tb.Sp.	Control	.0699	.00028	.0696	.0703
(mm)	Graft	.0439	.00415	.0387	.0490
2 week	Scl-Ab 100%	.0696	.00546	.0628	.0764
	Scl-Ab 75%	.0600	.00707	.0512	.0688
	Scl-Ab 50%	.0460	.00548	.0392	.0528
Tb.Sp.	Control	.0840	.00001	.0840	.0840
(mm)	Graft	.0500	.00001	.0500	.0500
4 week	Scl-Ab 100%	.0704	.00550	.0636	.0772
	Scl-Ab 75%	.0300	.00001	.0300	.0300
	Scl-Ab 50%	.0350	.00001	.0350	.0350

CBCT (cone-beam CT)—based volumetric measures from a standardized ROI around premolar sockets (24.63 mm²; alveolar crest to apex) to assess treatment effects on bone volume and microarchitecture. Outcomes: BV/TV (see Fig. 1), Tb.Th., Tb.Sp., at 2 and 4 weeks. ROI metrics were computed via an automated enclosing-convex-polygon workflow (modified BoneJ Density Distribution plugin for ImageJ), incorporating mass/density and concentric-density distributions. Groups (n = 5 per group): G1 Control (physiologic healing); G2 Graft (50 mg; right side = 2 weeks, left side = 4 weeks filled); G3 Scl-ab 100% (0.02 mg Scl-ab + 50 mg graft); G4 Scl-ab 75%; G5 Scl-ab 50% (both in 50 mg graft). Values are mean ± SD with 95% CI (n = number of animals). Abbreviations: CBCT: Cone-beam computed tomography; ROI: Region of interest; BV/TV: Bone volume/total volume; Tb.Th.: Trabecular thickness; Tb.Sp.: Trabecular separation; n: Number of animals; SD: Standard deviation; CI: Confidence interval; Scl-Ab: Sclerostin antibody.

Table 3. Between-group effects (Type III sums of squares) for BV/TV, Tb.Th., and Tb.Sp.

Source	Type III sum of squares	df	Mean square	F	Sig.	Partial Eta squared
BV/TV						
Intercept	14.680	1	14.680	29831.770	0.0001	.999
Groups	.580	4	.145	294.578	0.0001	.983
Error	.010	20	.000			
Tb.Th.						
Intercept	1.274	1	1.274	25788.769	0.0001	.999
Groups	.017	4	.004	84.457	0.0001	.944
Error	.001	20	4.941E-5			
Tb.Sp.						
Intercept	.156	1	.156	9139.569	0.0001	.998
Groups	.011	4	.003	157.851	0.0001	.969
Error	.000	20	1.708E-5			

The findings show that the group factor has a powerful effect on all BV/TV, Tb.Th., and Tb.Sp. parameters. All differences are highly statistically significant. The variance analysis between groups was conducted, and the main effect of the independent variable (group) on BV/TV, Tb.Th., and Tb.Sp. was evaluated. Abbreviations: BV/TV: Bone volume/total volume; Tb.Th.: Trabecular thickness; Tb.Sp.: Trabecular separation; df: Degrees of freedom.

Table 4. Multiple comparisons of BV/TV at 2 weeks

(I) Groups	(J) Groups	Mean			95% confide	ence interval
BV/TV	BV/TV	difference (I-J)	Std. Error	Sig.	Lower bound	Upper bound
Control	Graft	.10336*	.01384	0.0001	.0620	.1448
	Scl-Ab 100%	19430*	.01384	0.0001	2357	1529
	Scl-Ab 75%	10430*	.01384	0.0001	1457	0629
	Scl-Ab 50%	06830*	.01384	0.0010	1097	0269
Graft	Control	10336*	.01384	0.0001	1448	0620
	Scl-Ab 100%	29766*	.01384	0.0001	3391	2563
	Scl-Ab 75%	20766*	.01384	0.0001	2491	1663
	Scl-Ab 50%	17166*	.01384	0.0001	2131	1303
Scl-Ab 100%	Control	.19430*	.01384	0.0001	.1529	.2357
	Graft	.29766*	.01384	0.0001	.2563	.3391
	Scl-Ab 75%	$.09000^{*}$	.01384	0.0001	.0486	.1314
	Scl-Ab 50%	.12600*	.01384	0.0001	.0846	.1674
Scl-Ab 75%	Control	.10430*	.01384	0.0001	.0629	.1457
	Graft	.20766*	.01384	0.0001	.1663	.2491
	Scl-Ab 100%	09000*	.01384	0.0001	1314	0486
	Scl-Ab 50%	.03600	.01384	0.1080	0054	.0774
Scl-Ab 50%	Control	.06830*	.01384	0.0010	.0269	.1097
	Graft	.17166*	.01384	0.0001	.1303	.2131
	Scl-Ab 100%	12600*	.01384	0.0001	1674	0846
	Scl-Ab 75%	03600	.01384	0.1080	0774	.0054

<sup>\*</sup>The mean difference is significant at the 0.05 level (Tukey-HSD). Abbreviations: BV/TV: Bone volume/total volume; Scl-Ab: Sclerostin antibody.

Table 5. Multiple comparisons of BV/TV at 4 weeks

(I) Groups	(J) Groups	Mean			95% confide	nce interval
BV/TV	BV/TV	difference	Std.		Lower	Upper
		(I-J)	Error	Sig.	bound	bound
Control	Graft	.08640*	.00621	0.0001	.0616	.1112
	Scl-Ab	24160*	.00496	0.0001	2605	2227
	100%					
	Scl-Ab	15960*	.01577	0.0020	2284	0908
	75%					
	Scl-Ab	09960*	.01785	0.0220	1778	0214
	50%					
Graft	Control	08640*	.00621	0.0001	1112	0616
	Scl-Ab	32800*	.00735	0.0001	3538	3022
	100%					
	Scl-Ab	24600*	.01667	0.0001	3124	1796
	75%					
	Scl-Ab	18600*	.01865	0.0010	2617	1103
	50%					
Scl-Ab	Control	.24160*	.00496	0.0001	.2227	.2605
100%	Graft	.32800*	.00735	0.0001	.3022	.3538
	Scl-Ab	.08200*	.01625	0.0240	.0148	.1492
	75%					
	Scl-Ab	.14200*	.01828	0.0050	.0653	.2187
	50%					
Scl-Ab	Control	.15960*	.01577	0.0020	.0908	.2284
75%	Graft	.24600*	.01667	0.0001	.1796	.3124
	Scl-Ab	08200*	.01625	0.0240	1492	0148
	100%					

	Scl-Ab	.06000	.02362	0.1750	0219	.1419
	50%					
Scl-Ab	Control	.09960*	.01785	0.0220	.0214	.1778
50%	Graft	.18600*	.01865	0.0010	.1103	.2617
	Scl-Ab	14200*	.01828	0.0050	2187	0653
	100%					
	Scl-Ab	06000	.02362	0.1750	1419	.0219
	75%					

<sup>\*</sup> The mean difference is significant at the 0.05 level (Games-Howell test).

Abbreviations: BV/TV: Bone volume/total volume; Scl-Ab: Sclerostin antibody.

Table 6. Multiple comparisons of Tb. Th. at 2 and 4 weeks

Dependent	(I) Groups	(J) Groups	Mean			95% confiden	ce interval
variable			difference (I-				Upper
			J)	Std. Error	Sig.	Lower bound	bound
Tb.Th	. Control	Graft	.02708*	.00411	0.0090	.0098	.0444
(2		Scl-Ab	02778*	.00185	0.0001	0345	0211
(2		100%					
week)		Scl-Ab 75%	02018*	.00387	0.0220	0363	0040
		Scl-Ab 50%	01018	.00387	0.2090	0263	.0060
	Graft	Control	02708*	.00411	0.0090	0444	0098
		Scl-Ab	05486*	.00429	0.0001	0718	0379
		100%					
		Scl-Ab 75%	04726*	.00548	0.0001	0662	0283
		Scl-Ab 50%	03726*	.00548	0.0010	0562	0183
	Scl-Ab	Control	.02778*	.00185	0.0001	.0211	.0345
	100%	Graft	.05486*	.00429	0.0001	.0379	.0718
		Scl-Ab 75%	.00760	.00406	0.4250	0082	.0234

	_	Scl-Ab 50%	.01760*	.00406	0.0330	.0018	.0334
	Scl-Ab 75%	Control	.02018*	.00387	0.0220	.0040	.0363
		Graft	.04726*	.00548	0.0001	.0283	.0662
		Scl-Ab	00760	.00406	0.4250	0234	.0082
		100%					
		Scl-Ab 50%	.01000	.00529	0.3920	0083	.028
	Scl-Ab 50%	Control	.01018	.00387	0.2090	0060	.026
		Graft	.03726*	.00548	0.0010	.0183	.056
		Scl-Ab	01760*	.00406	0.0330	0334	001
		100%					
		Scl-Ab 75%	01000	.00529	0.3920	0283	.008
Tb.Th.	Control	Graft	.02252*	.00260	0.0040	.0110	.034
(4		Scl-Ab	03320*	.00184	0.0001	0413	025
(4		100%					
week)		Scl-Ab 75%	00880	.00375	0.2910	0254	.007
		Scl-Ab 50%	.00920	.00400	0.3050	0086	.027
	Graft	Control	02252*	.00260	0.0040	0340	011
		Scl-Ab	05572*	.00317	0.0001	0670	044
		100%					
		Scl-Ab 75%	03132*	.00455	0.0010	0475	015
		Scl-Ab 50%	01332	.00476	0.1360	0305	.003
	Scl-Ab	Control	.03320*	.00184	0.0001	.0251	.041
	100%	Graft	.05572*	.00317	0.0001	.0445	.067
		Scl-Ab 75%	.02440*	.00417	0.0070	.0086	.040
		Scl-Ab 50%	.04240*	.00440	0.0010	.0255	.059
	Scl-Ab 75%	Control	.00880	.00375	0.2910	0078	.025
		Graft	.03132*	.00455	0.0010	.0151	.047
		_		1	1	I	1

	Scl-Ab	02440*	.00417	0.0070	0402	0086
	100%					
	Scl-Ab 50%	.01800	.00548	0.0603	0009	.0369
Scl-Ab 50%	Control	00920	.00400	0.3050	0270	.0086
	Graft	.01332	.00476	0.1360	0038	.0305
	Scl-Ab	04240*	.00440	0.0001	0593	0255
	100%					
	Scl-Ab 75%	01800	.00548	0.0630	0369	.0009

Multiple comparisons were performed using the Games–Howell test. Abbreviations: Tb.Th.: Trabecular thickness; Scl-Ab: Sclerostin antibody; Std. Error: Standard error.

Table 7. Multiple comparisons of Tb. Sp. at 2 weeks

(I) Groups	(J) Groups	Mean difference			95% confidence	interval
		(i-j)	Std. Error	Sig.	Lower bound	Upper bound
Control	Graft	.02604*	.00319	0.0001	.0165	.0356
	Scl-Ab 100%	.00032	.00319	1.0000	0092	.0099
	Scl-Ab 75%	.00992*	.00319	0.0390	.0004	.0195
	Scl-Ab 50%	.02392*	.00319	0.0001	.0144	.0335
Graft	Control	02604*	.00319	0.0001	0356	0165
	Scl-Ab 100%	02572*	.00319	0.0001	0353	0162
	Scl-Ab 75%	01612*	.00319	0.0010	0257	0066
	Scl-Ab 50%	00212	.00319	0.9620	0117	.0074
Scl-Ab 100%	Control	00032	.00319	1.000	0099	.0092
	Graft	.02572*	.00319	0.0001	.0162	.0353
	Scl-Ab 75%	.00960*	.00319	0.0480	.0001	.0191
	Scl-Ab 50%	.02360*	.00319	0.0001	.0141	.0331
Scl-Ab 75%	Control	00992*	.00319	0.0390	0195	0004
	Graft –	.01612*	.00319	0.0010	.0066	.0257

	Scl-Ab 100%	00960*	.00319	0.0480	0191	0001
	Scl-Ab 50%	.01400*	.00319	0.0020	.0045	.0235
Scl-Ab 50%	Control	02392*	.00319	0.0001	0335	0144
	Graft	.00212	.00319	0.9620	0074	.0117
	Scl-Ab 100%	02360*	.00319	0.0001	0331	0141
	Scl-Ab 75%	01400*	.00319	0.0020	0235	0045

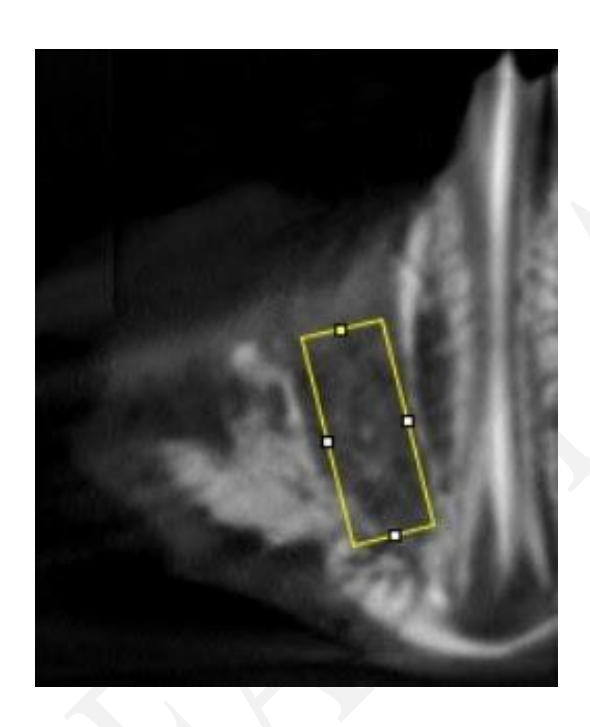
<sup>\*</sup>The mean difference is significant at the 0.05 level (Tukey HSD). Abbreviations: Tb.Sp.: Trabecular separation; Scl-Ab: Sclerostin antibody; Std. Error: Standard error.

Table 8. Multiple comparisons of Tb. Sp. at 4 weeks

(I) Groups	(J) Groups	Mean difference			95% confidence interval	
		(I-J)	Std. Error	Sig.	Lower bound	Upper bound
Control	Graft	.03400*	.00000	0.0001	.0340	.0340
	Scl-Ab 100%	.01360*	.00246	0.0240	.0027	.0245
	Scl-Ab 75%	.05400*	.00000	0.0001	.0540	.0540
	Scl-Ab 50%	.04900*	.00000	0.0001	.0490	.0490
Graft	Control	03400*	.00000	0.0001	0340	0340
	Scl-Ab 100%	02040*	.00246	0.0050	0313	0095
	Scl-Ab 75%	.02000*	.00000	0.0001	.0200	.0200
	Scl-Ab 50%	.01500*	.00000	0.0001	.0150	.0150
Scl-Ab 100%	Control	01360*	.00246	0.0240	0245	0027
	Graft	.02040*	.00246	0.0050	.0095	.0313
	Scl-Ab 75%	.04040*	.00246	0.0001	.0295	.0513
	Scl-Ab 50%	.03540*	.00246	0.0010	.0245	.0463
Scl-Ab 75%	Control	05400*	.00000	0.0001	0540	0540
	Graft	02000*	.00000	0.0001	0200	0200
	Scl-Ab 100%	04040*	.00246	0.0001	0513	0295

	Scl-Ab 50%	00500	.00000		0050	0050
Scl-Ab 50%	Control	04900*	.00000	0.0001	0490	0490
	Graft	01500*	.00000	0.0001	0150	0150
	Scl-Ab 100%	03540*	.00246	0.0010	0463	0245
	Scl-Ab 75%	.00500	.00000		.0050	.0050

<sup>\*</sup>The mean difference is significant at the 0.05 level (Games-Howell). Abbreviations: Tb.Sp.: Trabecular separation; Scl-Ab: Sclerostin antibody; Std. Error: Standard error.



**Figure 1. Standardized CBCT region of interest (ROI) for alveolar bone quantification.** Parasagittal CBCT slice of the mandibular premolar region. The ROI spans from the alveolar crest to the tooth apex and is fixed at 24.63 mm² for every specimen, enabling comparable extraction of BV/TV, Tb.Th., and Tb.Sp. Abbreviations: CBCT: Cone-beam computed tomography; ROI: Region of interest; BV/TV: Bone volume/total volume; Tb.Th.: Trabecular thickness; Tb.Sp.: Trabecular separation.

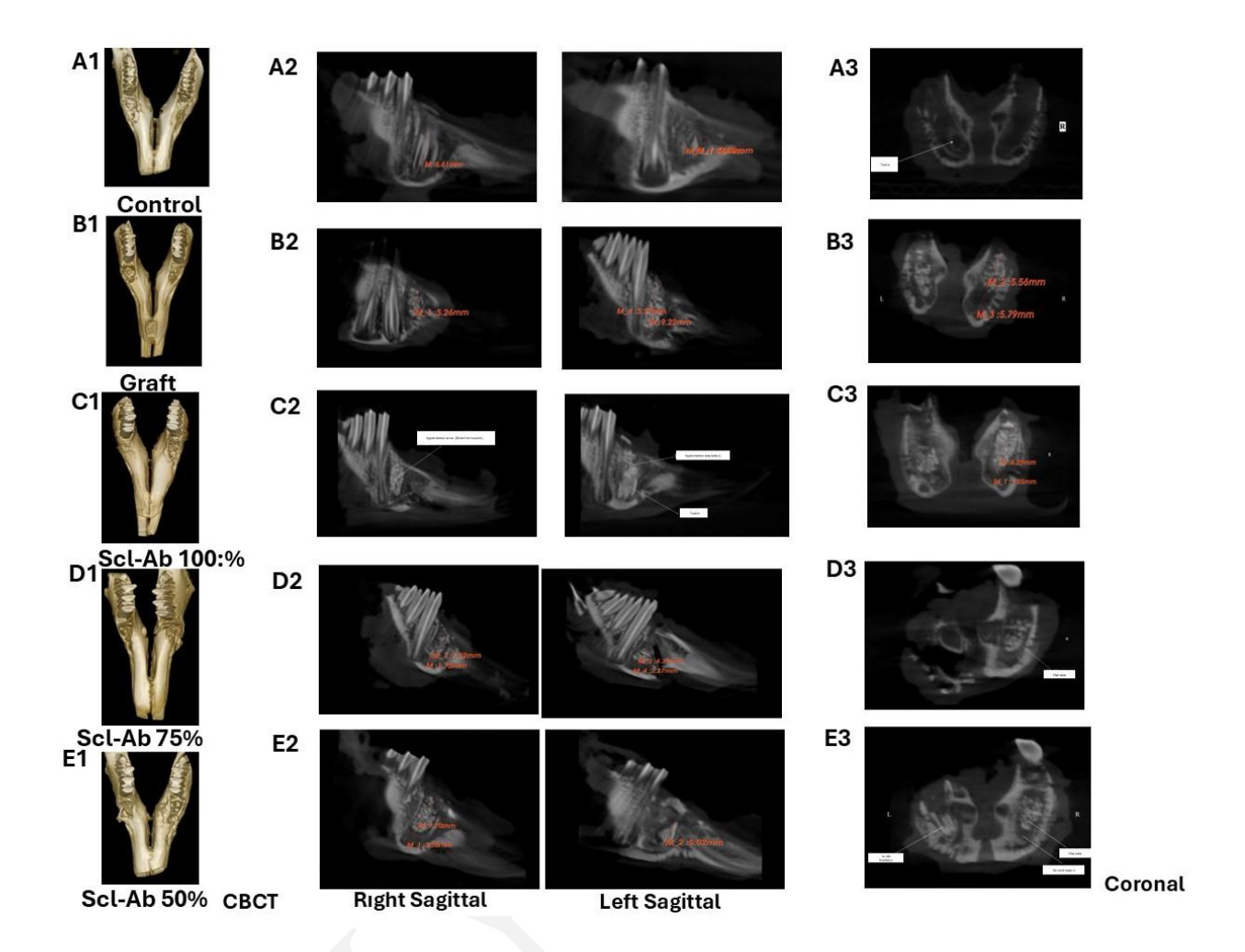


Figure 2. Selected 3D CBCT images: right sagittal views (2 weeks) and left sagittal views (4 weeks of treatment) for all groups. Cone-beam computed tomography (CBCT) was utilized to capture 3D images, as well as sagittal (A2–E2) and coronal views (A3–E3), at 2- and 4-week intervals across various treatment groups (control, graft, and Sclab). These images illustrate the differences in bone regeneration within the defect area, highlighting the visual variations in the extent of bone formation among the treatment modalities. Abbreviations: CBCT: Cone-beam computed tomography; Scl-ab: Sclerostin antibody.

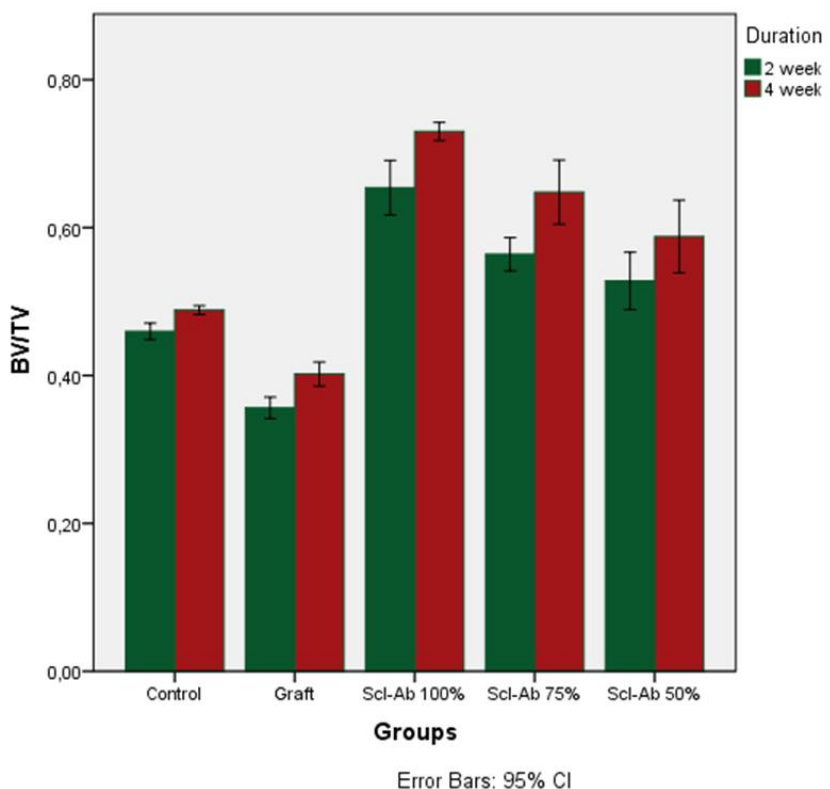


Figure 3. BV/TV ratios at two time points—week 2 (green bars) and week 4 (burgundy bars)—by treatment group. This comparison enables us to assess changes in bone volume over time. The images from the cone-beam computed tomography device were analyzed ex vivo and measured on axial, sagittal, frontal, and cross-sectional sections using the Cybermed On-Demand software, and further processed using CS 3D imaging software. Additionally, the region of interest chosen from the images was used to determine the volumetric analysis that covers a specific area of the field of view; volumetric measurements were taken on the selected alveolar bone surrounding the socket area of the extracted premolar tooth. Control: Only tooth extractions were done and left for physiological healing. Graft was placed after tooth extraction; the right and left sides were filled with 50 mg graft material. Scl-ab 100% represents 0.02 mg Scl-ab in 50 mg graft material, as a total dose, Scl-ab 75% and Scl-ab 50% in 50 mg graft material, and the ratio of Scl-ab. A significant difference was observed for BV/TV ratios within the groups during 2 and 4 weeks. Statistical significance was assessed using the Tukey and Games-Howell test. Abbreviations: BV/TV: Bone volume/total volume; Scl-ab: Sclerostin antibody.

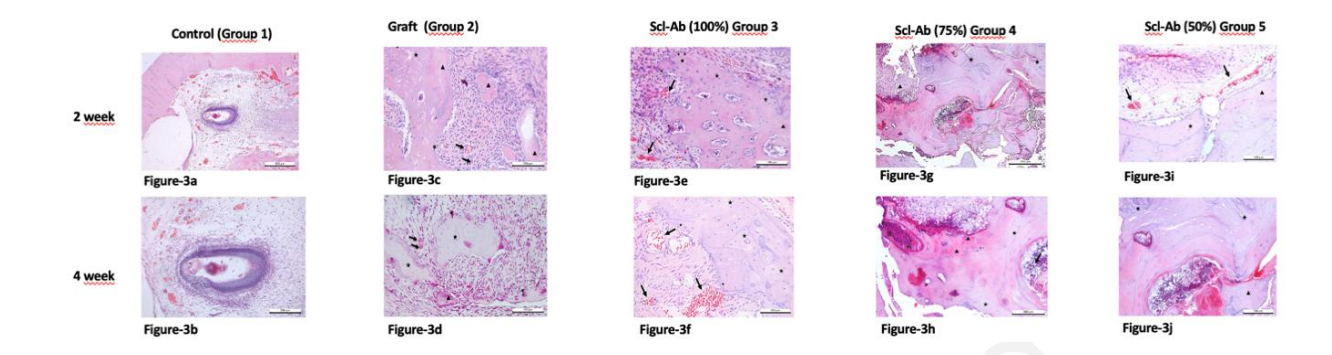


Figure 4. Histological comparison of socket healing in control, graft, and Scl-Ab groups. The sections were stained with hematoxylin and eosin (H&E). Figure 4c (100  $\mu$ m) indicates different stages of bone formation (early stage  $\triangle$ , advanced stage,  $\bigstar$ ). There was an increase in capillarization (indicated by the arrow). Osteoblasts were detected on the newly formed bone trabeculae's outer surface (\*). Figure 4d (100 µm): Capillary formations were observed less than in the graft 2w group (arrow). Bone trabeculae formation in different stages (early stage  $\triangle$ , advanced stage,  $\bigstar$ ) and multinucleated giant cells can be seen. All Scl-ab 2-week groups Figure 4e (100 μm), 4g (500 μm), 4i (100 μm): Areas where vascularization (arrow), osteoblasts (\*), and newly formed bone trabeculae (early stage ▲, advanced stage ★) are seen. Monitoring the graft in certain areas was evaluated by these findings (\*\*). All Scl-ab 4 weeks Figure 4f (100 μm), 4h (200 μm), 4j (100 μm); areas observed vascularization (arrow), newly formed bone trabeculae (early stage  $\triangle$ , advanced stage  $\bigstar$ ) are seen. This staining method allowed for visualising cellular and tissue structures, enabling us to assess the samples' healing processes and tissue organization. Control Group (Group 1), where only tooth extraction was performed, and the sites were allowed to undergo physiological healing for 2 (Figure 4a) and 4 (Figure 4b) weeks. Group 2, which involved graft application, yielded some intriguing results. The findings revealed that after four weeks, the level of capillarization was lower in the group that received the graft compared to the group that received it after 2 weeks. Abbreviation: Scl-ab: Sclerostin antibody.